

# QUASAR SPECTROSCOPY SONIFICATION: ANALYZING INTERGALACTIC AND CIRCUMGALACTIC MEDIA WITH SOUND

## ABSTRACT

In this paper, we present sonification approaches that enhance the exploration of matter residing in the intergalactic medium (IGM) and circumgalactic medium (CGM). As these media contain the majority of non-dark matter in the universe, astrophysicists are interested in investigating their material composition and relationship to the life and death of visible galaxies. Astrophysicists often analyze matter in these media using a technique called absorption line spectroscopy. Our sonification approaches convey key spectral features identified via this technique, including the presence and spread of spectral absorption lines within a region of the Universe, the relationship of a particular redshift location with respect to the absorption peak of a spectral absorption line, and the density of gas at various regions of the Universe. In addition, we present Quasar Spectrum Sound (QSS), a novel analysis tool that enables researchers to perform these sonification techniques on cosmological datasets, expanding the discovery and classification of matter in the IGM and CGM.

## 1. INTRODUCTION

Astronomical observations peering beyond the Milky Way have revealed billions of other galaxies in addition to our own. These galaxies are primarily detected by the starlight they emit. However, the matter detectable via emission from stars represents a small fraction of the matter that composes the Universe, even when we neglect the contribution of dark matter, which dominates the matter budget [1]. Indeed, the majority of “normal” matter (consisting of protons, neutrons, and electrons) resides *outside* the luminous starlit regions of galaxies, within the circumgalactic medium (CGM) and intergalactic medium (IGM) [2, 3, 4, 5].

This material is theorized, and empirically supported, to comprise ionized gas that is so diffuse it is undetectable through the light it emits. Rather, this tenuous gas must be detected via absorption line spectroscopy. This technique involves observing a bright emitting source in the distant universe, such as a quasar, obtaining a spectrum (wherein the object’s light is dispersed into its constituent wavelengths). Foreground complexes of gas leave a signature on the spectrum wherein light from the background source is removed at specific wavelengths corresponding to the atomic energy transitions of chemical species (atoms and ions) found in the gas “cloud”. Because these transition wavelengths are set by well-understood atomic physics, species such as neutral hydrogen have characteristic spectral “fingerprints” that enable the chemical composition of intergalactic and circumgalactic gas to be identified.

Astrophysicists study the IGM and CGM for a myriad of reasons. The majority of non-dark matter is purported to reside in the IGM and CGM, and there is an ongoing initiative to obtain a census of this ionized gas to validate predictions from the prevailing cosmological theories [6, 7, 8]. Furthermore, understanding the chemical composition of this gas can constrain models of how elements such as carbon, oxygen, magnesium, and iron (those with atomic number greater than helium) propagate throughout the Universe [9, 10]. Lastly, IGM and CGM gas play critical roles in the evolution of galaxies. Gas flows from the IGM and CGM are galaxies’ “lifeline”, as they cannot form new generations of stars without them [11, 12]. Conversely, the explosive deaths of stars expel matter and energy from galaxies into the CGM and IGM, modulating the mass, temperature, and density of gas within galaxies [13, 14]. Any self-consistent theory of how galaxies form and evolve must reproduce conditions in the CGM/IGM.

From the observational perspective, the task at hand centers on first identifying and then analyzing the absorption lines in spectra. Identifying IGM and CGM spectral lines essentially involves two key properties: the chemical species and the velocity at which the detected gas complex is moving. The former is generally determined by the aforementioned spectral energy transitions set by atomic physics. As the gas is predominately ionized, one typically encounters species such as O VI, C IV, or Mg II. In this nomenclature, an ion is denoted by the atomic symbol of the element then a numeral indicating the ionization state. For example, O I represents neutral oxygen (equal numbers of electrons and protons), O II is singly ionized oxygen (one electron stripped away), and O VI denotes an oxygen nucleus with five electrons missing.

The second key property of an absorption line is the velocity of the gas it traces. The velocity is reflected in analogy to the Doppler effect, where sound waves emitted from a source in relative motion to an observer appear to decrease or increase in frequency. In spectroscopy, lines from an absorbing or emitting source with relative motion to the observer will appear *redshifted* or *blueshifted* and occur at longer or shorter wavelengths, respectively, than the characteristic wavelengths of their atomic transitions. For this reason, we will refer to these characteristic wavelengths as *rest-frame wavelengths*.

Below, we present our sonification approach to the analysis of quasar spectroscopy, emphasizing how sonification can augment and accelerate the study of IGM and CGM. Specifically, we introduce four techniques to: *a)* identify presence of spectral absorption lines, *b)* characterize the spread of spectral absorption lines within a region of the Universe, *c)* compare the qualities of a particular redshift location with respect to the absorption peak of a specified spectral absorption line, and *d)* highlight the density of gas at various regions of the Universe. We also discuss details of *Quasar Spectrum Sound* (QSS), our interactive software tool that encapsulates these sonification techniques, enabling researchers to investigate cosmological datasets.



This work is licensed under Creative Commons Attribution Non-Commercial 4.0 International License. The full terms of the License are available at <http://creativecommons.org/licenses/by-nc/4.0>

## 2. BACKGROUND AND RELATED WORK

Sonification has made numerous appearances in the realms of both astronomy and spectroscopy. In both fields, it has been shown to provide a complementary perspective to existing analysis techniques and enhance discovery.

### 2.1. Astronomy

In the field of astronomy, sonification has demonstrated the ability to lead to new discoveries, enhance visual representations, and broaden the accessibility of data analytics. For example, as the Voyager 2 space probe was traveling across the rings of Saturn there was a problem with the space craft. The problem could not be discerned with visual controls due to the large amount of noise present in the signal. However, when realized aurally through a digital synthesizer, a salient sonic pattern emerged described as a “machine gun” sound. This led to the discovery that the problem was caused by collisions with electromagnetically charged micrometeoroids [15].

In 2009, Greg Laughlin, an astronomer at the University of California, Santa Cruz developed a sonification tool called *Systemic* that helps researchers to detect of extra-solar planets from data acquired by the Kepler Telescope. The tool uses a range of data analysis techniques in tandem with sonification, and potential planetary orbits can be identified from the harmonics in the sonified data [16].

In 2012, Alexander et al. demonstrated success audifying data from the Solar Wind Ion Composition Spectrometer. While listening to the raw solar data, they detected an underlying “hum” at a frequency of 137.5 Hz. Upon closer inspection, it was discovered that the sound corresponded to solar rotations and had implications for the carbon ion composition of solar winds. The harmonics in the tone present indicated periodic changes in temperature and hence solar wind type, allowing for the study of the temporal evolution of the Sun’s wind source regions [17].

The blind astronomer Wanda Diaz Merced has performed considerable research in data sonification related to space physics data. Diaz Merced sonified data using the tool *xSonify*, first created at the NASA Goddard Space Flight Centre and later converted to a user-centered prototype at the University of Glasgow in Scotland. In her 2013 PhD thesis, she summarizes the organization of focus groups to test her sonifications with the tool, finding that it gives scientists a better understanding of the data [18].

### 2.2. Spectroscopy

Sonification has also exhibited many unique representations in the field of spectroscopy, ranging from pure audification to musical composition. Newbold et al. [19] and Morowitz [20] have sonified the structure of molecules through the audification of Nuclear Magnetic Resonance (NMR) spectra. An NMR spectrum plots the spectral intensity of a chemical shift, and peaks present in the spectrum are converted directly into the frequencies of sinusoids in an audio signal. Each chemical has a unique spectrum and, thus, a unique sound when audified. This procedure has shown to be advantageous as it allows for fast and efficient detection of chemicals present in large amounts of data.

Similar to the above approach, Terasawa et al. [21] present a sonification of ECOG Seizure Data where the data are parameter mapped to overtones in a sound spectrum. The authors label

this approach as “gestalt formation” operating as a means of applying semantics to sound. In the approach, the overall timbre of a sonority is a representation or display of features, where the spectral characteristics of the sound signify the characteristics of the source. In their implementation, fifty-six channels of ECOG data were monitored. To sonify the data, a fundamental frequency of 180 Hz was selected, and sixteen harmonics of sinusoids were realized. Each harmonic was then amplitude modulated by each channel of ECOG data.

Pietrucha [22] takes a musically based parameter mapping approach in his sonification of spectra. In this approach, plots of absorption vs wavelength are presented, where spectral peaks in terms of absorption strength are mapped to frequency. The wavelength at which the peak is present is represented by a chord, where the harmonic quality of the chord indicates its location along the wavelength axis. The domain of wavelengths is divided into bands, where wavelengths residing in the shortest band are represented by a tonic chord, and subsequent bands utilize other diatonic chords, such as the subdominant, dominant, or submediant. The result is highly musical, with a melodic succession representing peak intensities that is accompanied by a chord progression representing wavelength location.

The *Atom Tone* project explores aesthetic possibilities for spectral sonification through music composition. Sonic material is generated through synthesis and modulation. Tones are generated via the audification of atomic emission spectra similar to the NMR approach above. The generated tones are then modified via effects processing techniques such as waveshaping, frequency shifting, or filtering, where the modification parameters are based on data taken from the periodic table of elements. The modulation is conceptually more open-ended, with the goal being for the musician to find the most aesthetically pleasing result and to have many options to explore [23].

Finally, Martin et al. [24] devised an approach to allow the visually impaired to examine audio spectrograms. With this sonification, a user is instructed to first select a frequency band to be monitored, and then set a threshold level in decibels. If a spectral peak in the selected band exceeds the threshold, a short beep will sound, where the frequency of the beep corresponds to the decibel level above the threshold.

## 3. QUASAR SPECTROSCOPY SONIFICATION

Here, we present a sonification approach to the analysis of quasar spectroscopy, with particular applications to studying the IGM/CGM in mind. Our main goal in sonifying quasar spectra is to detect gas in the IGM and CGM and localize it in velocity. To accomplish this, we search for absorption signatures of spectral lines that correspond to particular ions we seek. As discussed in Section 1, our primary observational technique for studying the IGM/CGM is via absorption lines in spectra to background quasars. Each quasar spectrum probes the IGM/CGM gas along the line of sight, and the observables for each spectrum include a flux and uncertainty value for each wavelength recorded at the detector. Before sonification, the data are reduced, all exposures are coadded, and we normalize the flux by dividing by an approximation to the intrinsic shape of the quasar itself (the continuum). Hereon, we will simply refer to the normalized flux as ‘flux’. The flux will take on values ranging from 0 to 1, where smaller flux values indicate stronger absorption signatures. The location of each absorption feature is determined by the velocity of the gas. As this

velocity is dominated by the expansion of the Universe, shifting spectral lines to longer (redder) wavelengths, we generally quantify this velocity first by a *redshift*  $z$ :

$$\lambda_{\text{obs}} = \lambda_{\text{rest}}(1 + z) \quad (1)$$

where  $\lambda_{\text{obs}}$  is the wavelength at which a feature is observed and  $\lambda_{\text{rest}}$  is the rest frame wavelength of the spectral transition.

### 3.1. Presence of Absorption

The primary feature we aim to sonify is the presence of a spectral absorption line. Certain ions present within a gas cloud may have multiple signature transitions ( $\lambda_{\text{rest}}$ ) for which our data have spectral coverage; each spectrum covers a particular range of ( $\lambda_{\text{obs}}$ ). To corroborate the identification of a given ion, we attempt to scan for up to three lines from the ion. Certain ions may have more than three lines covered in our spectra, and in this case, we scan for the three lines with the highest absorption probabilities (determined by atomic physics).

In sonifying absorption presence, we first assign each spectral line to a particular sonic frequency, where each frequency constitutes a tone of a major triad. We call this frequency the *presence frequency*. The spectral line with the highest absorption probability is assigned to the root of the triad, the second highest probability is mapped to the interval a perfect fifth above the root, and the final line is mapped to the major third of the triad.

In addition, each tone of the triad is assigned a unique timbre. The root is designated as a sine tone, the fifth is a square wave, and the third is a sawtooth wave [25]. Assigning a unique timbre to each tone allows them to be more easily delineated [26], which is important as we try to listen to qualities of each tone simultaneously.

Next, the amplitude for each tone is determined by the amount of absorption present in a corresponding line. At a given redshift, we map the flux at that pixel to amplitude as follows:

$$A = 1 - F_{rs} \quad (2)$$

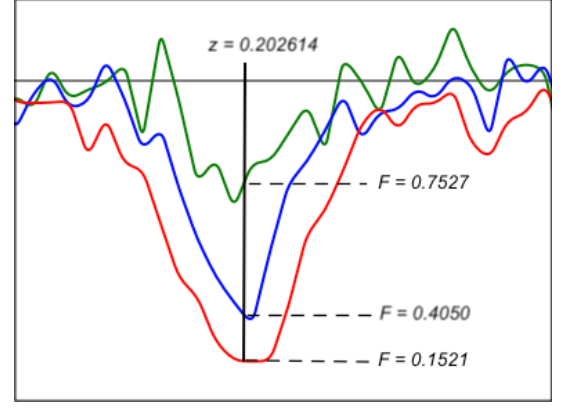
where  $F_{rs}$  is the flux obtained for a spectral line at a given pixel, denoted by the redshift (see Figure 1). Thus, as the absorption increases, the chord tone for the associated line becomes more pronounced.

As a user scans through the spectrum in redshift space searching for the presence of a particular ion, each chord tone varies in intensity. For ions with three spectral lines covered by the data, the goal is for the user to find a location (in redshift) where they hear the full presence of the major triad. If the user hears the simultaneous presence of every chord tone, then they have potentially identified the location of the ion they seek.

It is important for the user to not only listen for the presence of the absorption lines but also to listen to the balance of amplitude among the tones present. The spectral transitions should exhibit a unique proportion of absorption among the lines (once again set by atomic physics), and the overall mix of the triadic tones should reflect this relationship.

### 3.2. Absorption Linewidth

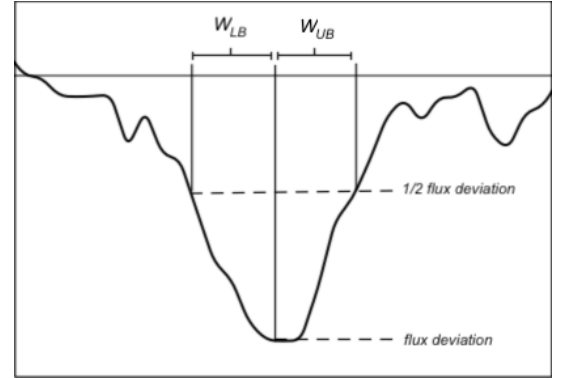
The width of each absorption line is also sonified, reflecting the spread of absorption present and asymmetry in the absorption profile. We determine the absorption width as the upper and lower



Absorption Feature Alignment for Neutral Hydrogen

Figure 1: Alignment of absorption lines (shifted to their rest frames and superimposed) for H I at a redshift  $z$  of 0.202614. The flux value for the first spectral line (red) is 0.1521 (amp = 0.8479), the second line (blue) is 0.4050 (amp = 0.595), and the third (green) is 0.7527 (amp = 0.2473).

bound wavelengths that correspond to half the flux deviation from 1.0 observed at a given redshift (see Figure 2).



Spectral Absorption Width

Figure 2: An absorption line with width at 1/2 the flux deviation from 1 for a given redshift. The total width is divided into upper and lower sections centered about the current red shift.

For this sonification, a dual tone, bi-directional glissando is produced that represents the overall width and skewness of the absorption signature. First, we determine the bounding tones of the glissando. For each line, the spectral width upper and lower bounds are mapped to frequencies that are above and below the presence frequency. The glissando tones simultaneously emerge from this base and then sweep the frequency space until arriving at their respective boundaries. The width of the absorption, as represented by the glissandi, is characterized by duration and distance. A broader absorption line will have glissandi that cover a wider sonic frequency range and is longer in duration. Moreover, each glissando differ in duration. This is an indication of asymmetry (or skewness) in the absorption width. For example, if one glissando is longer in duration traversing the higher frequency than

the lower, then the upper bound of the absorption is proportionally further from the line center than the lower bound. The skewness of the absorption is an important feature to perceive, as it may indicate that our scan is not centered at the absorption peak, or it may indicate contamination from absorption of a different ion at a different redshift.

### 3.3. Centroiding

Upon detecting the presence of a particular spectral transition, we can perform centroid sonification. This allows us to hear how well aligned the currently scanned redshift location is with respect to the absorption peak. To accomplish this, for each line we introduce a centroid tone and compare it to the presence tone. As with the spectral linewidth, we compute a neighborhood about the current redshift and then determine upper and lower bound wavelengths at half of the flux deviation at our redshift location. With the absorption width calculated, we then compute the ratio between the widths above and below the current redshift. The centroid tone is then introduced, whose frequency is the presence frequency multiplied by the calculated ratio:

$$f_{centroid} = f_p \frac{W_{UB}}{W_{LB}} \quad (3)$$

where  $f_p$  is the presence frequency for the spectral line,  $W_{UB}$  is the upper bound absorption width, and  $W_{LB}$  is the lower bound absorption width.

If our redshift is centralized about the current absorption area, the ratio between upper and lower bound widths will equal 1, causing the centroid frequency and presence frequency to sound in unison. If not, the added tone will form a dissonance that is above or below our tone of reference. If the centroid tone sounds higher in pitch, then we are positioned above the absorption center and can adjust downwards to find the line centroid. If the centroid tone sounds lower, then we can re-position upwards to centroid. In addition to the coarser scanning in redshift space, our framework allows a finer scanning at smaller velocity intervals (recall that the redshift is merely an expression of velocity due to the Universe's expansion). As one adjusts the velocity of the reference tone, they can hear the quality of the dissonance between the tones change. The dissonance heard is characterized as beating or roughness between the two tones. As we deviate away from the centroid, the beating increases in frequency causing a rough sonority. The user can finely adjust the velocity position of our reference tone, listening for the beating to slow until the roughness diminishes and a unison forms.

### 3.4. Apparent Column Density

As stated above, the various absorption lines associated with a particular ion will have differing characteristic strengths. We can adjust for these differing intrinsic absorption strengths using the apparent optical depth at each pixel, from which we then calculate the Apparent Column Density (ACD). Savage and Sembach present the method in great detail [27], but the ACD is essentially intended to reflect the density of gas intercepted along the line of sight in particular region of space. Therefore, comparing the ACD in each pixel for multiple spectral lines can be used to verify that our detected absorption profiles match for the ions we seek.

When observing a given spectral transition at a particular redshift, ACD relates its oscillator strength, restframe wavelength,

and absorption such that when this relationship is compared among all spectral transitions for a given ion, they should be equal. We calculate the ACD for each absorption line as follows:

$$ACD \propto \frac{1}{O_s \lambda_{rest}} \ln\left(\frac{1}{F}\right) \quad (4)$$

where, for a given ion,  $O_s$  is the oscillator strength,  $\lambda_{rest}$  is the rest-frame wavelength, and  $F$  is the absorbed flux, in terms of flux at a given redshift. If the calculated ACD for all spectral lines covered for a given ion are equal, then this is strong validation we have accurately identified an ion.

To sonify the ACD, we first compare the percentage change in ACD between successive absorption lines as follows:

$$\Delta ACD_n = \frac{ACD_n}{ACD_{n-1}} - 1 \quad (5)$$

where  $ACD_n$  is the apparent column density for spectral line  $n$ . Then, the ACD frequency for a given absorption line is calculated as:

$$f_{ACD} = f_p \times 2^{\Delta ACD \frac{1}{6}} \quad (6)$$

where  $f_p$  is the presence frequency for a given spectral line, and  $\Delta ACD$  is the ACD percentage change for the line.

The user hears the ACD frequency in comparison to the presence frequency assigned to the spectral transition. If the ACD for a particular transition aligns with the others, then the ACD frequency will sound in unison with the base. If it is not, a dissonance will be heard. Thus overall, when listening the presence of all spectral lines at a given redshift, if they all align in presence as well as in absorption (proportionally), a fully in-tune triad will sound.

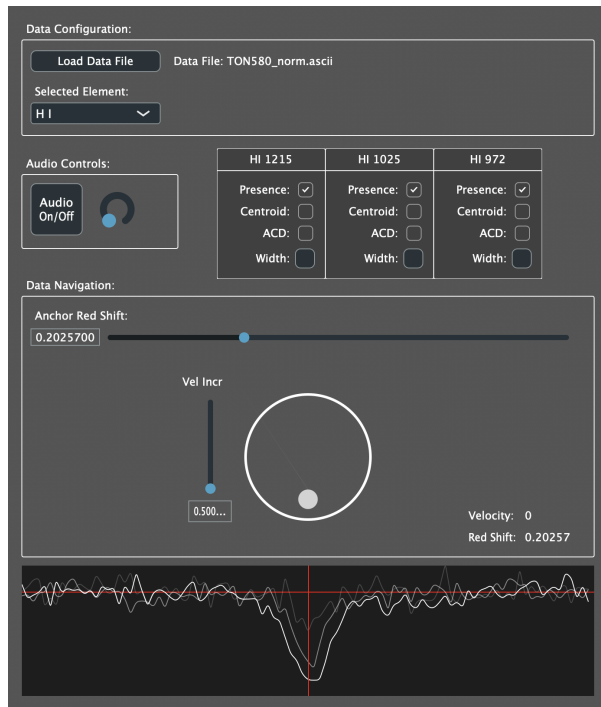
## 4. QSS SOFTWARE

We developed the software Quasar Spectroscopy Sound (QSS) as an analysis tool for detecting gaseous ions in the intergalactic and circumgalactic medium. The software largely utilizes Juce, a C++ based API, for its user interface and audio processing. The sonification audio results from an ensemble of direct digital signal processing techniques, all developed in C++. The user interface consists of three sections to assist in performing analysis: Data Configuration, Audio Controls, and Data Navigation.

### 4.1. Data Configuration

The Data Configuration section allows the user to import a desired data set and select an ion for spectral analysis. Quasar spectrum data sets may be obtained from the Hubble Spectroscopic Legacy Archive (HSLA) [28] among other sources. As mentioned above, each spectrum includes the intrinsic signature of the quasar itself. This needs to be removed in order to reveal the net absorption or emission signatures in the spectrum. Thus each spectrum, once downloaded from the HSLA, was preprocessed using the linetools software package [29]. We fit a continuum over the full wavelength range of the spectrum, then normalize the data by dividing by the continuum, and extract the normalized spectrum as an ASCII table with the parameters of wavelength, flux, and error.

Upon importing the data set the user may select a individual ion for analysis. The ions available for selection are derived from the atomic data set compiled by Verner et al. [30]. This data set



(a) QSS User Interface

Figure 3: The QSS software user interface with sections including Data Configuration (top), Audio Controls (upper middle), Data Navigation (bottom middle), and spectral absorption plot (bottom).

contains ion names and their spectral transition properties of rest-frame wavelength, oscillator strength, and an absorption probability, which we use for data filtration.

As our aim is to focus on absorption systems most commonly encountered outside of our galaxy, we filter out ions and spectral transitions that are least likely to be found (informed by past experience analyzing similar data through traditional techniques) in the IGM/CGM gas we are studying. We omit ions that are considered to be fine-structure and excited-state, as these materials are mainly observed residing in our galaxy. In addition, we filter on the properties of absorption probability and rest-frame wavelength, only importing spectral transitions with an absorption probability greater than 9.75 and with wavelengths between 900 and 1800 Angstroms, commensurate with the spectral coverage of the *Hubble Space Telescope* instrument that collected the data. Finally, we aim to analyze only three spectral transitions for a given element. If a particular element has more than three spectral transitions that meet our initial criteria, we only preserve the spectral transitions with the three highest absorption probabilities.

#### 4.2. Audio Controls

The Audio Controls section includes standard controls to enable playback and control the overall volume level of the audio. To the right of these controls are boxes that allow the user to control audio features of the spectral sonification. Each of these boxes identifies the spectral transition of an element by element name and rest-frame wavelength. The first of the controls is a “Presence” toggle button for listening to the absorption presence. Enabling this al-

lows the users to hear the absorption strength, perceived in terms of amplitude, of the spectral line present at a selected redshift. Next, there is a “Centroid” button that, when enabled, allows the user to hear the positioning of the selected redshift with respect to the spectral width as described in Section 3.3. Third, an “ACD” toggle button enables the sonification for apparent column density, allowing the user to hear how a given spectral transition is aligned with respect to others of the same ion. Finally, there is a “Width” trigger button. Clicking on this button triggers a glissando that represents the absorption linewidth for given neighborhood in redshift.

#### 4.3. Data Navigation

The Data Navigation section consists of user interface widgets that allow the user to scan the spectral data and a visual spectral plot. First and foremost, at the top of the section, the user sets a redshift anchor by either entering a value in the number box or adjusting the horizontal slider that encompasses the redshift range of the ion being analyzed. Scrubbing the data via redshift alone can be problematic as even small increments in redshift account for large changes in velocity, which can cause the user to skip over sections in the data too quickly and thus miss many absorption features. Thus, in addition to the slider, we have included a velocity jog wheel that allows the user to scrub the data at finer level of detail. With this tool, the user can explore the absorption in the neighborhood of a local spectral region at varying intervals ranging from velocity increments of 0.1 to 25 meters per second. The jog wheel is essential for exploring the centroid, width, and apparent column density sonifications.

Directly underneath the navigation widgets is a visual plot of the spectral data. The plot appearing in the window shows the spectral neighborhood about the currently selected red shift. The absorption lines for (up to) all three spectral transitions are superimposed, allowing the user to more easily see areas of absorption alignment. This visualization appeals to more traditional spectral analysis techniques and enhances data navigation while serving as a complement to the sonification.

### 5. RESULTS AND FUTURE WORK

Initial analyses using quasar spectroscopy sonification with the QSS software have shown potential to be a valuable resource for intergalactic and circumgalactic medium science. Currently, the prevalent tools available for analysis reside in the visual realm, and the addition of a sonic perspective has the ability to not only enhance current more visually oriented tools but also stand alone as a methodology and provide unique advantages. For example, it became immediately clear early in the development process that QSS can enable more rapid discovery and identification of IGM/CGM system candidates than visually scanning through spectra. In addition, early testing indicates that hearing the presence of absorption features can improve sensitivity to weaker lines, as it can be challenging to visually identify these weak lines among the noise. These advantages combine to greatly increase the discovery space in re-analyzing already existing archival data as well as in anticipation of the next generation spectroscopic surveys on the horizon.

Although our sonification approaches and software have already undergone substantial development iterations based on expert feedback, we now are seeking additional feedback from a broader user community made up of astrophysicists with varying specializations and at different career stages to further enhance the

methodology and its applications. In addition, we are building on the framework developed here to extend spectral sonification approaches to other realms of scientific analysis, e.g., connecting the properties of CGM absorption (sonified) to properties (i.e., star formation rate and mass) of the galaxies themselves hosting the gas we ‘hear’.

A demo of the QSS software is attainable via the project repository located at <https://github.com/CreativeCodingLab/QuasarSonify>.

## 6. REFERENCES

- [1] M. Fukugita and P. J. E. Peebles, “The Cosmic Energy Inventory,” *The Astrophysical Journal*, vol. 616, no. 2, pp. 643–668, Dec. 2004.
- [2] J. Tumlinson, M. S. Peebles, and J. K. Werk, “The Circumgalactic Medium,” *Annual Review of Astronomy and Astrophysics*, vol. 55, pp. 389–432, Aug. 2017.
- [3] M. McQuinn, “The Evolution of the Intergalactic Medium,” *Annual Review of Astronomy and Astrophysics*, vol. 54, pp. 313–362, Sept. 2016.
- [4] J. N. Burchett, D. Abramov, J. Otto, C. Artanegara, J. X. Prochaska, and A. G. Forbes, “IGM-Vis: Analyzing intergalactic and circumgalactic medium absorption using quasar sightlines in a Cosmic Web context,” *Computer Graphics Forum*, vol. 38, no. 3, pp. 491–504, June 2019.
- [5] J. N. Burchett, O. Elek, N. Tejos, J. X. Prochaska, T. M. Tripp, R. Bordoloi, and A. G. Forbes, “Revealing the dark threads of the Cosmic Web,” *The Astrophysical Journal Letters (ApJL)*, vol. 891, no. 2, p. L35, March 2020.
- [6] R. Cen, J. Miralda-Escudé, J. P. Ostriker, and M. Rauch, “Gravitational collapse of small-scale structure as the origin of the Lyman-alpha forest,” *The Astrophysical Journal Letters*, vol. 437, pp. L9–L12, Dec. 1994.
- [7] R. Davé, R. Cen, J. P. Ostriker, G. L. Bryan, L. Hernquist, N. Katz, D. H. Weinberg, M. L. Norman, and B. O’Shea, “Baryons in the warm-hot intergalactic medium,” *The Astrophysical Journal*, vol. 552, pp. 473–483, May 2001.
- [8] J. Tumlinson, C. Thom, J. K. Werk, J. X. Prochaska, T. M. Tripp, N. Katz, R. Davé, B. D. Oppenheimer, J. D. Meiring, A. B. Ford, J. M. O’Meara, M. S. Peebles, K. R. Sembach, and D. H. Weinberg, “The COS-Halos survey: Rationale, design, and a census of circumgalactic neutral hydrogen,” *The Astrophysical Journal*, vol. 777, p. 59, Nov. 2013.
- [9] L. L. Cowie, A. Songaila, T.-S. Kim, and E. M. Hu, “The metallicity and internal structure of the Lyman-alpha forest clouds,” *Astronomical Journal*, vol. 109, pp. 1522–1530, Apr. 1995.
- [10] J. N. Burchett, T. M. Tripp, J. X. Prochaska, J. K. Werk, J. Tumlinson, J. M. O’Meara, R. Bordoloi, N. Katz, and C. N. A. Willmer, “A Deep Search For Faint Galaxies Associated With Very Low-redshift C IV Absorbers: II. Program Design, Absorption-line Measurements, and Absorber Statistics,” *The Astrophysical Journal*, vol. 815, no. 2, p. 91, 2015.
- [11] R. B. Larson, “Infall of Matter in Galaxies,” *Nature*, vol. 236, pp. 21–23, Mar. 1972.
- [12] D. Kereš, N. Katz, D. H. Weinberg, and R. Davé, “How do galaxies get their gas?” *Monthly Notices of the Royal Astronomical Society*, vol. 363, pp. 2–28, Oct. 2005.
- [13] S. Veilleux, G. Cecil, and J. Bland-Hawthorn, “Galactic winds,” *Annual Review of Astronomy and Astrophysics*, vol. 43, pp. 769–826, Sept. 2005.
- [14] D. Fielding, E. Quataert, M. McCourt, and T. A. Thompson, “The impact of star formation feedback on the circumgalactic medium,” *Monthly Notices of the Royal Astronomical Society*, vol. 466, pp. 3810–3826, Apr. 2017.
- [15] G. Kramer, B. Walker, T. Bonebright, P. Cook, J. H. Flowers, N. Miner, and J. Neuhoﬀ, “Sonification report: Status of the field and research agenda,” 2010.
- [16] G. Laughlin. (2012) Systemic: Characterizing planets. [Online]. Available: <http://oklo.org>
- [17] R. L. Alexander, J. A. Gilbert, E. Landi, M. Simoni, T. H. Zurbuchen, and D. A. Roberts, “Audification as a diagnostic tool for exploratory heliospheric data analysis,” in *Proceedings of the International Community on Auditory Display (ICAD)*, 2011.
- [18] W. L. D. Merced, “Sound for the exploration of space physics data,” Ph.D. dissertation, University of Glasgow, 2013.
- [19] J. W. Newbold, A. Hunt, and J. Brereton, “Chemical spectral analysis through sonification,” in *Proceedings of the International Community on Auditory Display (ICAD)*, 2015.
- [20] F. Morawitz, “Molecular sonification of nuclear magnetic resonance data as a novel tool for sound creation,” in *Proceedings of the International Computer Music Conference (ICMC)*, 2016, pp. 6–11.
- [21] H. Terasawa, J. Parvizi, and C. Chafe, “Sonifying ecog seizure data with overtone mapping: A strategy for creating auditory gestalt from correlated multichannel data,” in *Proceedings of International Community on Auditory Display (ICAD)*, 2012.
- [22] M. Pietrucha, “Sonification of spectroscopy data,” Ph.D. dissertation, Worcester Polytechnic Institute, 2019.
- [23] J. Suchánek, “ATOM TONE v2.0—software for sonification of atomic data for purpose of electroacoustic music,” in *Proceedings of the International Symposium on Sound*, 2018.
- [24] F. Martin, O. Metatla, N. Bryan-Kinns, and T. Stockman, “Accessible spectrum analyser,” in *Proceedings of the International Community on Auditory Display (ICAD)*, 2016.
- [25] M. Puckette, *The theory and technique of electronic music*. World Scientific Publishing Company, 2007.
- [26] D. Huron, “A derivation of the rules of voice-leading from perceptual principles,” *The Journal of the Acoustical Society of America*, vol. 93, no. 4, pp. 2362–2362, 1993.
- [27] B. D. Savage and K. R. Sembach, “The analysis of apparent optical depth profiles for interstellar absorption lines,” *The Astrophysical Journal*, vol. 379, pp. 245–259, 1991.
- [28] M. Peebles, J. Tumlinson, A. Fox, A. Aloisi, S. Fleming, R. Jedrzejewski, C. Oliveira, T. Ayres, C. Danforth, B. Keeney, et al., “The Hubble Spectroscopic Legacy Archive,” *Instrument Science Report COS*, vol. 4, 2017.

- [29] J. X. Prochaska, et al., “linetools/linetools: Third minor release,” Oct. 2017. [Online]. Available: <https://doi.org/10.5281/zenodo.1036773>
- [30] D. Verner, G. J. Ferland, K. Korista, and D. Yakovlev, “Atomic data for astrophysics. II. New analytic fits for photoionization cross sections of atoms and ions,” *arXiv preprint astro-ph/9601009*, 1996.